HHS Public Access

Author manuscript

Am J Surg Pathol. Author manuscript; available in PMC 2018 December 01.

Published in final edited form as:

Am J Surg Pathol. 2017 December ; 41(12): 1642–1656. doi:10.1097/PAS.0000000000000940.

Solitary Fibrous Tumors of the Head and Neck: A Multi-Institutional Clinicopathologic Study

Steven C. Smith, M.D., Ph.D.[1,2,3], **William E. Gooding, M.S.**[4], **Matthew Elkins, M.D., Ph.D.**[5], **Rajiv M. Patel, M.D.**[3,6], **Paul W. Harms, M.D., Ph.D.**[3,6], **Andrew S. McDaniel, M.D., Ph.D.**[3], **Nallasivam Palanisamy, Ph.D.**[7], **Cora Uram-Tuculescu, M.D.**[1], **Bonnie B. Balzer, M.D., Ph.D.**[2], **David R. Lucas, M.D.**[3], **Raja R. Seethala, M.D.**[8,*], and **Jonathan B. McHugh, M.D.**[3,9,*]

[1]Departments of Pathology and Surgery, VCU School of Medicine, Richmond, VA, USA

[2]Department of Pathology and Laboratory Medicine, Cedars-Sinai Medical Center, Los Angeles, CA, USA

[3]Department of Pathology, University of Michigan Health System, Ann Arbor, MI, USA

[4]Biostatistics Facility, University of Pittsburgh Cancer Institute, Pittsburgh, PA, USA

[5]Department of Pathology, SUNY Upstate Medical University, Syracuse, NY, USA

[6]Department of Dermatology, University of Michigan Health System, Ann Arbor, MI, USA

[7]Department of Urology, Henry Ford Health System, Detroit, MI, USA

[8]Department of Pathology, University of Pittsburgh Medical Center, Pittsburgh, PA, USA

[9]Department of Oral and Maxillofacial Surgery, University of Michigan Health System, Ann Arbor, MI, USA

Abstract

Solitary fibrous tumors (SFTs) of the head and neck are uncommon. Lesions previously diagnosed in the head and neck as hemangiopericytomas (HPCs), giant cell angiofibromas (GCAs), and orbital fibrous histiocytoma (OFHs) are now recognized as within the expanded spectrum of SFTs. To better understand the clinicopathologic profile of head and neck SFTs, we performed a multi-institutional study of 88 examples. There was no sex predilection (F:M ratio 1.2), and the median patient age was 52y (range 15>89). The sinonasal tract and orbit were the most common sites involved (30% and 25%), followed by the oral cavity and salivary glands (15% and 14%). Original diagnoses included HPC (25%), SFT (67%), and OFH (6%), with one SFT and one OFH noted as showing GCA-like morphology. On review, the predominant histologic pattern was classic SFT-like in 53% and cellular (former HPC-like) in 47%; lipomatous differentiation (8%) and giant cell

Corresponding Author: Steven Christopher Smith, M.D., Ph.D. Assistant Professor, Assistant Director of Surgical Pathology, Department of Pathology, Virginia Commonwealth University School of Medicine, 1200 E. Marshall Street, PO Box 980662, Richmond, VA, 23298 USA, Tel +1-804-828-4918, fax +1-828-8733, steven.c.smith@vcuhealth.org.

*Both authors share senior authorship for this work.

Disclosures/Note: A preliminary analysis of this project was presented as an oral proffered paper at the 102nd United States and Canadian Academy of Pathology Annual Meeting in Baltimore, MD, March 2013, for which it was awarded the 2013 Vincent Hyams Award from the North American Society of Head and Neck Pathology.

The authors declare there are no conflicts of interest.

angiofibroma-like pattern (7%) were less prevalent. Subsets demonstrated nuclear atypia (23%), epithelioid morphology (15%), or coagulative necrosis (6%). Infiltrative growth (49%) and osseous invasion (82%) were prevalent among evaluable cases. Of the 48 SFTs with follow-up (median 77mo, mean 100mo), 19 showed recurrence (40%). Of these, four patients were alive with disease and four dead of disease. Size and mitotic rate were negative prognosticators using a joint prognostic proportional hazards regression model. Three patients experienced metastasis, to lungs, parotid, bone, and skull base, including one case showing overtly sarcomatous “dedifferentiation”. As a group, SFTs present in a wide anatomic and morphologic spectrum in the head and neck. Only rare examples metastasize or cause death from disease. However, the fairly high local recurrence rate underscores their aggressive potential and highlights the importance of prospective recognition.

Keywords

solitary fibrous tumor; hemangiopericytoma; orbital fibrous histiocytoma; giant cell angiofibroma; STAT6

Introduction

The concepts of solitary fibrous tumor (SFT) and hemangiopericytoma (HPC) have evolved significantly between their first descriptions in the pleura in 1931 (1) and in various sites in 1942 (2) and their unification as SFT in contemporary WHO classifications (3, 4). The SFT spectrum of neoplasms is believed to be composed of specialized fibroblasts, arises in diverse anatomical sites, and exhibits protean histomorphology. However, the diagnosis is best made through appreciation of bland, ovoid to spindle cells haphazardly arrayed in a “patternless pattern” of varying cellular density in admixture with stromal collagen bundles and arranged around characteristic “staghorn” vasculature. The histologic spectrum has expanded with appreciation of myxoid (5), epithelioid (6, 7), and lipomatous (8-10) SFTs, as well as identification of cases showing atypical features (5, 11, 12) and sarcomatous dedifferentiation (6, 13, 14). Despite the histologic diversity, recent molecular findings confirm the identity of these lesions through their shared pathognomonic genetic lesion, oncogenic fusion of the genes *NAB2* and *STAT6* (15-19), detectable by sequencing, PCR, FISH among a subset, or simply by immunohistochemistry .

Prior published series suggest that classic SFTs of the head and neck represent ~6% of all SFTs, or approximately one quarter of extrathoracic SFTs, which in turn represent one quarter of all SFTs (12, 20-23). Thus, limited data describe the biologic potential of these unpredictable lesions in the distinctive clinical and anatomic milieu of the head and neck. Moreover, lesions previously designated as giant cell angiofibroma (GCA) and orbital fibrous histiocytoma (OFH) have been recently proposed to be part of the spectrum of SFTs (24) and may alter the overall anatomic distribution or prognosis. Conversely new molecular data confirm the exclusion from SFT of head and neck specific lesions, including the true pericytic neoplasm, glomangiopericytoma or sinonasal HPC (25, 26), has been recently found exhibit *CTNNB* mutation and nuclear accumulation of β-catenin (27). Additionally,

the recently described, biphenotypic low-grade sinonasal sarcoma with neural and myogenic features (28, 29), deserves mention as a newer entity outside of the SFT spectrum.

This rapid evolution of morphologic and molecular understanding in this area calls for a reassessment of the contemporary spectrum of head and neck SFTs, especially to better define their biologic potential and clinical behavior. Herein, we report findings from this retrospective analysis, which consists of consecutive cases encountered over a number of years at the hospitals of the University of Michigan, the University of Pittsburgh, Cedars-Sinai Medical Center, and Virginia Commonwealth University.

Methods

Multi-Institutional Retrospective Case Series

With Institutional Review Board approval from participating institutions, searches were performed using the laboratory information systems of the University of Michigan Health System (UMHS; 1990-2013) University of Pittsburgh Medical Center (UPMC; 1982-2015), Cedars-Sinai Medical Center (CSMC 1990-2014), and VCU Health System (1990-2014) cases diagnosed previously as SFT, HPC, GCA, and OFH. Archival slides and or tissue blocks were obtained from institutional slide libraries, and H&E-stained recuts were performed if paraffin blocks were available. Consultation cases were included if material were retained and available for evaluation (predominantly, UPMC). De-identified clinical data were tabulated, including sex, age (censored at >89 years), anatomic site, and follow-up status regarding local recurrence or metastasis, from the electronic medical record and pathology department files.

Histologic Review

Cases previously diagnosed as SFT, HPC, GCA and OFH, identified by retrospective searches, were included for review if they were judged clinically to have arisen in mesenchyal tissues of the head and neck, above the clavicle. Cases clinically considered to be primary to the central nervous system were excluded from consideration, given the differing anatomic and surgical aspects. For morphologic inclusion criteria, only tumors that met the morphologic definition used by the WHO Classification of Tumors of Soft Tissue, 4th edition, as described for the entity, e*xtrapleural solitary fibrous tumor* (3) (and briefly defined for the morphologic patterns below), were included for study. All other non-SFT entities, e.g., glomangiopericytoma, synovial sarcoma, and biphenotypic sinonasal sarcomas were excluded (consensus review of histology and available molecular findings by SCS, ME, and JBM).

Pathologic parameters tabulated included original diagnostic term, largest gross dimension, overall histologic pattern and presence or absence of atypia, lipomatous differentiation, myxoid/microcystic change, epithelioid morphology, infiltrative growth, and bone invasion, each defined below. Mitoses per 10 high power fields were counted in the most cellular areas. The overall histologic pattern was defined as “classic SFT” if the lesion showed a predominant pattern of low-to-moderate cellularity of spindle cells interspersed within a prominently collagenized matrix. Cases showing areas of focally increased cellularity were

still defined as “classic SFT”, if such areas were not the predominant pattern. Lesions were defined as a “cellular SFT” if the predominant histologic pattern was of a densely cellular proliferation of ovoid-to-spindled cells arrayed in a “patternless pattern” within a less prominent stroma. Atypia was defined as *nuclear atypia*, which included coarse chromatin, anisonucleosis, more than mild pleomorphism, and/or nuclear overlap. Any amount of unequivocal lipomatous differentiation was sufficient to consider it as present. Epithelioid morphology was defined by a pervasive pattern of round to polygonal cells with ample clear-to-pale, or eosinophilic cytoplasm and nuclei with macronucleoli; scattered foci or foci of clear cell change were excluded from this designation. Infiltrative growth was scored as present if a lesion showed even focal infiltration of perilesional adipose or soft tissue (if present for evaluation), or if a tumor showed invasion around native ductal structures (if present for evaluation). Bone invasion was considered present even if focal in cases where resected tissue included bone for evaluation. All slides were reviewed by three pathologists (SCS, ME, JBM) blinded to clinical and outcome parameters.

Immunohistochemistry

Available archived immunohistochemically (IHC) stained slides were reviewed and tabulated if interpretable (SCS and JBM). For UMHS cases where archival CD34 IHC stains were not available or interpretable, IHC for CD34 was performed on selected sections in the UMHS Clinical Immunohistochemistry Core. These studies used monoclonal clone QBEnd10 (Dako, Carpenteria, CA) at 1:100 dilution after pretreatment with CC1 buffer (Dako) for 30 minutes at 95 Celsius on a Benchmark Ultra autostainer (Ventana, Tucson, AZ). STAT6 IHC was performed on UMHS, CSMC, and VCUHS cases using an antibody to the protein Cterminus (SC-621, Santa Cruz, Biotechnology, Dallas TX) at a 1:200 dilution using ultraView DAB detection kit (760-500; Ventana Medical Systems/Roche, Tucson, AZ) and hematoxylin counterstain on a BenchMark XT autostainer (Ventana). STAT6 IHC was performed at UPMC using rabbit monoclonal STAT6 antibody (Clone YE361; Abcam, Cambridge MA, 1:500) on a Leica Bond III. STAT6 IHC was considered positive if present in a nuclear distribution within 10% or more of lesional cells, as reported previously (18), while CD34 IHC was scored by proportion of tumor cells positive as 0 (negative), 1+ (focal or multifocal), or 2+ (diffuse), both by SCS and JBM.

Statistical Analysis

Time to disease recurrence was defined as elapsed time between diagnosis and disease recurrence. Patients without disease were censored as of their last date of follow-up or date of death if dying from a cause other than SFT. Probability of recurrence was estimated by the Kaplan-Meier method with Greenwood confidence interval. A panel of demographic, treatment related and histologic factors were examined for effect upon time to recurrence with proportional hazards regression. A parsimonious (i.e., composed of the fewest number of parameters necessary to explain the outcome) multivariate model was developed from individual covariates. Assumptions of linearity were tested for the continuous variables (tumor size, mitotic index) and the proportional hazards assumption was verified for the final model. Computations were made with the software package, R (30) using the package, rms (31).

Results

Cohorts

Database searches and histologic review of cases of SFT, HPC, OFH, and GCA resulted in a cohort of 88 cases from UMHS (n=30, 34%), UPMC (n=37, 42%), CSMC (n=11, 13%), and VCUHS (n=10, 11%).

Clinical Characteristics

Table 1 lists clinical findings by case. Median age at diagnosis was 52y with a range of 15 to >89 years. The most prevalent primary site of involvement was the sinonasal tract (n=26; 30%), of which the nasal cavities were involved in 77% (Figure 1A), the paranasal sinuses in 31%, and additionally the skull base in 23%. Second in prevalence to the sinonasal ones were SFTs arising primarily in the orbit (n=22; 25%); of these, three extended to clinically involve the lacrimal gland (14%), while two eroded into the skull base (9%). Next in prevalence were tumors based in the oral cavity (n=13, 15%), which involved buccal soft tissue in nearly half (n=6; 46%), followed by the tongue (n=3, 23%), palate (n=2, 15%), and the masseter and peritonsilar soft tissues (one each). Next in prevalence were SFTs arising in the major salivary glands (n=12; 14%), ten of which arose in the parotid (83%), and two in the submandibular gland (17%). Eight tumors (9%) arose in the deep tissues of the neck, of which four were parapharyngeal and one more supraclavicular, arising in the deep musculature of the neck base, extending caudad from above the clavicle (Figure 1B-C). One final neck SFT arose in the periphery of the thyroid gland. Minor subsets of the SFTs were predominantly clinically documented as based in the subcutaneous soft tissues (n=6; 7%), of which three involved the cheek, and two involved the eyelids. A single SFT arose in the external auditory canal.

Pathologic Characteristics

Original versus Contemporary Diagnoses—Original diagnoses included “hemangiopericytoma” (n=22; 25%), “solitary fibrous tumor” (n=59; 67%), and OFH (n=5; 6%). None had a topline diagnosis of GCA, though two cases (1% each) documented GCA-like features, one of which was originally diagnosed as an OFH and the other of which was diagnosed as a HPC. With regard to classic versus cellular morphology, there was a high degree of concordance between original diagnosis and contemporary classification, such that 19/22 (86%) of “hemangiopericytomas” corresponded to cellular SFT and 39/59 (66%) cases corresponded to classic SFT, $p<0.001$. Of the OFHs, 3 showed classic SFT morphology, while 2 showed cellular morphology; of the OFH and SFT with previously noted GCA-like areas, both showed classic morphology.

Gross and Microscopic Features—Head and neck SFTs were described macroscopically as circumscribed, solid, indurated, fibrous lesions, that were white, tan, or grey in color, while a case with lipomatous differentiation was softer with a “fish flesh” appearance. One SFT that demonstrated dedifferentiation into an overt high-grade sarcoma showed an infiltrative, multinodular appearance with copious necrosis described on the cut surfaces, see Figure 2. Specimens from primary tumors ranged from 0.4cm to 9.7cm, with a

median of 2.8cm. Among recurrent lesions, the size ranged from 0.4cm to 10cm, median 4.5cm.

Histologically, classic SFT morphology was observed more frequently (n=47, 53%) than cellular SFT (n=41, 47%), Figure 3. Atypia, present as increased nuclear pleomorphism and/or coarseness of chromatin was present in 20 (23%), while epithelioid cytomorphology was observed in 13 (15%), see Figure 4. Additional morphologic variations noted included lipomatous differentiation, which was observed in seven SFTs (8%), and stromal giant cells such as described in GCA were seen in six (7%), Figure 5. Areas of myxoid change with cystic or microcystic morphology was noted in six (7%), which coincided with lipomatous differentiation in two of the six. Nodular hyaline deposits reminiscent of collagen rosettes were noted in four (5%), Figure 6, while an unusual pattern of predominant paucicellular sclerotic collagen was apparent in one sinonasal SFT.

Of 69 evaluable cases, infiltrative growth, defined as either an infiltrative border or as infiltration around entrapped native structures such as epithelial elements and ducts, was apparent in 34 (49%), while of SFTs where bone was included in histologic sections, 14/17 (82%) demonstrated osseous invasion. Coagulative tumor cell necrosis was noted in five (6%), while mitoses ranged from 0 to 18 per 10 high power fields, with a median of 1. Dedifferentiation, present as overtly malignant, undifferentiated high-grade sarcomatous transformation with frank pleomorphism and ~50% necrosis was identified in a single SFT. Infiltrative and aggressive patterns seen are shown in Figure 7.

Immunohistochemical stains included most frequently CD34, which was available for 80 cases, of which 41 (51%) showed strong, diffuse CD34 positivity and a further 32 (40%) showed focal to multifocal positivity. These and additional immunohistochemical findings tabulated from re-review of archival material are summarized by Table 2 and Figure 8. In light of recent observation of a recurrent, pathognomic *NAB2-STAT6* gene fusions present in SFTs (15-17), we performed STAT6 immunohistochemistry on all cases from CSMC and VCUHS (n=21), and reviewed STAT6 findings for a subset of UMHS cases (n=12) (18) and UPMC cases (n=12). All were positive for STAT6 in a nuclear distribution, including lesions previously designated as OFH, and the conventional SFT areas of the case with dedifferentiation.

Recurrence – Free Survival and Clinicopathologic Factors—Among the 88 patients whose pathologic characteristics were described previously, follow up for disease recurrence was available for 48 (55%). In particular, follow-up was lacking in 24 of the 37 (65%) of patients collected at UPMC, which was related to inclusion for morphologic review of a large number of consultation cases from patients treated at outside institutions. Also, the original diagnosis of HPC was overrepresented in the followed patients, although this appears to be random variation rather than systematic. According to a recursive partitioning model, patients with follow-up did differ those without follow-up, predominately due to institutional differences. No differences were seen in variables that predicted recurrence, leading to the conclusion that analysis of factors associated with recurrence did not compromise results.

Among the 48 patients followed up with observation (median 77 months, mean 100 months), 19 recurrences, mainly locoregional, were noted. Among the 29 patients who were disease free, the median follow-up time was 43 months (range 0 – 274 months). Median time to recurrence (Figure 9) was 10 years, though 12 of 19 recurrences occurred within 2.5 years. Three patients experienced distant metastases, one of which (orbital primary site) had lung and parotid metastases. One additional patient had lung metastasis (the dedifferentiated SFT based in lower neck deep soft tissue) and additional metastases to the skull base. One final patient developed bone metastases. Six SFTs (13%) had documentation of multiple known recurrences (median 3.5, range: 2-7). Four patients (8%) died of disease.

Factors associated with recurrence were investigated with proportional hazards regression (see Table 3). Size (p=0.04, HR=1.68), atypia (p=0.01, HR=3.44), mitotic rate (overall p=0.06, HR=1.67), necrosis (p=0.02, HR=4.98), and epithelioid cytomorphology (p=0.05, HR=2.56) were risk factors for recurrence. In an additive joint prognostic model, size (p=0.08, HR=1.63) and mitoses >4 per 10 high power fields (p<0.01, HR=1.79) were associated with risk of recurrence (LR chi square = 10.64, 2df p<0.01).

Discussion

Experience with this large cohort of head and neck SFTs sheds important light on several aspects of this disease, including a changing morphologic and anatomic range in the head and neck, with associated issues in the histopathologic differential diagnosis. Most importantly, however, this cohort provides sufficient experience with cases to allow useful observations regarding pathologic features associated with prognosis for SFTs at this site. Once again, the prognostic associations observed in this cohort echo longstanding ideas about SFTs, only with uniquely differing applications in the setting of the head and neck surgery and surgical pathology.

First, regarding the morphologic and anatomic range of SFTs in the head and neck, our study confirms some prior findings and challenges others. Comparing our experience with perhaps the most comprehensive review of all published head and neck SFT cases as of 2010, sourced from the oral pathology literature (32), overall, we confirmed a lack of proclivity for female or male patients and similar median age (52 years) and size (2.8cm). In terms of anatomic range, however, our cohort confirmed our suspicion that inclusion of OFHs and GCAs in the SFT spectrum – as supported by nuclear STAT6 expression seen in all cases we studied – results in a significant overall proportion (25%) of head and neck SFTs arising in the orbit compared to the 6% reported previously (32). These findings establish the orbital primary site as nearly as frequent as the sinonasal tract (30%), a discordance we feel reflects more limited access to non-oral sites by oral pathologists and publication biases in an area previously dominated by case reports and small series.

The overall differential diagnosis of SFTs, given the variations in cellularity and stromal changes, is quite broad, encompassing a number of benign and malignant entities, and has been reviewed extensively elsewhere (20, 33). Speaking to the more anatomically specific differential in the head and neck, during review of these tumors, especially myxoid, cystic, and lipomatous ones (5, 11, 34), we saw raised diagnostic consideration of entities with

significantly different treatments and prognoses from SFTs. For example, one tumor with extensive myxoid and lipomatous differentiation, had presented in consultation with a prior diagnosis of “myxoid neoplasm, favor sarcoma” with consideration of a diagnosis of a high-grade myxoid liposarcoma. Break-apart FISH for the *FUS* locus had been performed (and was negative). While challenging on the original biopsy material, the resection demonstrated diagnostic features of SFT (and confirmatory STAT6 positivity), supporting the utility of this marker in this setting. Another example is that of the thyroid SFT identified in our review. While scattered case reports (35-37) and one smaller series (38) describe SFTs arising in the thyroid and its capsule, our experience of only one among 88 lesions studied confirms the rarity of this presentation. Awareness of our recent observation of positivity for PAX8 (and to a lesser extent, PAX2) in nearly a third of SFTs of diverse sites (39) is important. In the head and neck, PAX8 has become a workhorse marker for thyroid carcinomas, including anaplastic (40), the latter consideration having been proposed for our thyroid case at preoperative aspiration. One additional case actually raised the unusual differential of an amyloidoma (41). This exceptionally sclerotic and hypocellular SFT had been studied by Congo red (and was negative), though STAT6 was positive, as were diagnostic histologic features.

Most useful, to our mind, are the prognostic observations to be made from this cohort. The clinical behavior of SFTs, generally, remains difficult to predict based on traditional histopathologic parameters, and much of the published literature regarding these lesions focuses on tumors with either HPC (42-44) or SFT (12, 21, 45) morphology. The large, recent cohort from Demicco *et al.*, describes a series of 110 cases, including both SFTs and HPCs, from a variety of anatomic sites, usefully including 12 from the head and neck (46). Based on review of their (entire) cohort, a model was proposed based on age, size, and mitotic index, for stratification of SFTs for overall risk of *metastasis and death*. They observed that small tumors with low mitotic rates were very unlikely to metastasize, while large tumors (≥ 15 cm) in patients ≥ 55 years of age with mitotic figures of ≥ 4/10 HPFs required close follow-up due to a high risk of metastasis and death from disease (46). Though we routinely employ the Demicco model in our practice for SFTs of other sites, we underscore that this model is of limited use, operationally, for head and neck SFTs. As an illustration of why this is the case, consider the relative rarity of metastases (6%) yet frequent local recurrences (36%) in our cohort as compared to much higher rates of metastases (26%) and lower rate of local recurrences (10%) in the overall Demicco cohort (46). (For that matter, head and neck SFT sizes rarely pass 5 cm, let alone 15 cm). In short, our experience suggests that the overall clinical outcome of head and neck SFTs is driven by *recurrence, which is predominantly local*.

Modeling, then, recurrence, on unconditional univariate analysis we found that atypia, size, mitotic rate, epithelioid morphology and necrosis were adverse prognostic factors for head and neck SFTs, closely echoing the classic criteria for malignancy in HPC proposed by Enzinger and Smith (mitotic rate, size, hypercellularity, cellular pleomorphism, hemorrhage, and necrosis) (42). Interestingly, size and mitotic rate cut-offs suggested by analysis of the interquartile range from 25th to 75th percentile also very closely approximated the originally proposed cut-offs, namely >4 mitoses per 10 high power fields, and 5 cm. In a joint prognostic model it appears that both size and mitotic index remain jointly prognostic for

recurrence. Thus, overall, we note that that the parameters of size and mitotic index, albeit with slightly different cutoffs, associated with risk of metastasis in prior SFT cohorts (42, 46), actually are associated with local recurrence in the head and neck. Thus, we recommend careful assessment of these parameters for prospective assessment of head and neck SFTs, and in our ongoing clinical practice note their association with aggression.

One more disappointing potential prognostic parameter in the cohort was margin status: we observed overall a high rate of histologically positive margins (67%) that did not correlate with local recurrence. We speculate that this finding may relate to the unique aspects and challenges of head and neck surgery, and emphasize, as we have reported previously (47), that overall margin status must be assessed with close surgical and pathologic correlation. Endoscopic resections may show SFT extending broadly to cauterized margins yet may be deemed operatively free based on three-dimensional anatomy. Such is borne out in our data, where in tumors with both follow-up and interpretable margins, 17% with apparently negative margins recurred locally, while 52% with positive margins did not.

We acknowledge that compared to prior head and neck SFTs cohorts, the recurrence rate we observed was higher. Prior studies report recurrence in 2 of 13 (48), 0 of 11 (32), 1 of 12 (49), 2 of 8 (50), or 2 of 29 (51) head and neck SFTs, though these smaller series had predominantly shorter median follow-up. Even among a consecutive series of 9 histologically malignant solitary fibrous tumors of the head and neck reported by Yang *et al.* only 3 recurred (52), still less than the 36% we observed. In contrast, our data are more in keeping with the head and neck subset of the MD Anderson series reported by Demicco *et al.* (local recurrence in 3/12, metastasis in 2/12) (46), with the caveat that both this cohort and ours may equally reflect referral center bias. Even so, we echo the observations of Demicco *et al.* regarding the need for long-term follow-up for these cases. We observed recurrences as late as 228, 130, and 120 months, a phenomenon that has been noted in head and neck SFTs previously (51); our median time to recurrence was 19 months.

In summary, our findings confirm that SFTs of the head and neck demonstrate the full morphologic spectrum of these tumors at other sites, recognizing an expanded anatomic range including many orbital examples related to reclassification of lesions as SFT. Several of these cases that presented diagnostic challenges underscore particular diagnostic difficulties in the head and neck, ranging from PAX8 positivity, to myxoid and lipomatous patterns, to densely sclerotic SFTs. Overall, SFTs of the head and neck have a substantial local recurrence rate, indeed exceeding that seen for SFTs at other sites, but only infrequent ones metastasize or cause death from disease. The high rate of local recurrence underscores the intermediate malignant potential of these tumors and the need for long-term follow-up.

Acknowledgments

The authors would like to thank Dr. Javed Siddiqui of the Michigan Center for Translational Pathology and Dr. Jorge Almenara of VCU Health System Anatomic Pathology for laboratory support for recuts for review of archival SFT cases. This project used the UPCI Biostatistics Facility that is supported in part by award P30CA047904. This project was also supported in part by SPORE Grant U54CA168512 to RMP.

References

1. Klemperer P, Rabin CB. Primary neoplasm of the pleura: a report of five cases. Arch Pathol. 1931; 11:385–412.
2. Stout AP, Murray MR. Hemangiopericytoma: a vascular tumor featuring Zimmerman's pericytes. Ann Surg. 1942; 116:26–33. [PubMed: 17858068]
3. Fletcher, CDM., Bridge, JA., Lee, JC. Extrapleural solitary fibrous tumor. In: Fletcher, CDM.Bridge, JA.Hogendoorn, PCW., et al., editors. WHO classification of tumours of soft tissue and bone. Lyon: IARC Press; 2013. p. 80-82.
4. Guillou, L., Fletcher, JA., Fletcher, CDM., et al. Extrapleural solitary fibrous tumor and haemangiopericytoma. In: Fletcher, CDM.Unni, KK., Mertens, F., editors. Pathology and genetics of tumours of soft tissue and bone. Lyon: IARC Press; 2002. p. 86-90.
5. de Saint Aubain Somerhausen N, Rubin BP, Fletcher CD. Myxoid solitary fibrous tumor: a study of seven cases with emphasis on differential diagnosis. Mod Pathol. 1999; 12:463–471. [PubMed: 10349983]
6. Mosquera JM, Fletcher CD. Expanding the spectrum of malignant progression in solitary fibrous tumors: a study of 8 cases with a discrete anaplastic component--is this dedifferentiated SFT? Am J Surg Pathol. 2009; 33:1314–1321. [PubMed: 19718788]
7. Wetzel WJ. Solitary fibrous tumor. Hum Pathol. 1996; 27:513–514. [PubMed: 8621192]
8. Nielsen GP, Dickersin GR, Provenzal JM, et al. Lipomatous hemangiopericytoma. A histologic, ultrastructural and immunohistochemical study of a unique variant of hemangiopericytoma. Am J Surg Pathol. 1995; 19:748–756. [PubMed: 7793472]
9. Lee JC, Fletcher CD. Malignant fat-forming solitary fibrous tumor (so-called “lipomatous hemangiopericytoma”): clinicopathologic analysis of 14 cases. Am J Surg Pathol. 2011; 35:1177–1185. [PubMed: 21716088]
10. Guillou L, Gebhard S, Coindre JM. Lipomatous hemangiopericytoma: a fat-containing variant of solitary fibrous tumor? Clinicopathologic, immunohistochemical, and ultrastructural analysis of a series in favor of a unifying concept. Hum Pathol. 2000; 31:1108–1115. [PubMed: 11014579]
11. Dantey K, Cooper K. Myxoid solitary fibrous tumor: a study of three cases. Int J Surg Pathol. 2013; 21:358–362. [PubMed: 23248341]
12. Nielsen GP, O'Connell JX, Dickersin GR, et al. Solitary fibrous tumor of soft tissue: a report of 15 cases, including 5 malignant examples with light microscopic, immunohistochemical, and ultrastructural data. Mod Pathol. 1997; 10:1028–1037. [PubMed: 9346183]
13. Subramaniam MM, Lim XY, Venkateswaran K, et al. Dedifferentiated solitary fibrous tumour of the nasal cavity: the first case reported with molecular characterization of a TP53 mutation. Histopathology. 2011; 59:1269–1274. [PubMed: 22026427]
14. Thway K, Hayes A, Ieremia E, et al. Heterologous osteosarcomatous and rhabdomyosarcomatous elements in dedifferentiated solitary fibrous tumor: further support for the concept of dedifferentiation in solitary fibrous tumor. Ann Diagn Pathol. 2013; 17:457–463. [PubMed: 23040384]
15. Robinson DR, Wu YM, Kalyana-Sundaram S, et al. Identification of recurrent NAB2-STAT6 gene fusions in solitary fibrous tumor by integrative sequencing. Nat Genet. 2013; 45:180–185. [PubMed: 23313952]
16. Chmielecki J, Crago AM, Rosenberg M, et al. Whole-exome sequencing identifies a recurrent NAB2-STAT6 fusion in solitary fibrous tumors. Nat Genet. 2013; 45:131–132. [PubMed: 23313954]
17. Mohajeri A, Tayebwa J, Collin A, et al. Comprehensive genetic analysis identifies a pathognomonic NAB2/STAT6 fusion gene, nonrandom secondary genomic imbalances, and a characteristic gene expression profile in solitary fibrous tumor. Genes Chromosomes Cancer. 2013; 52:873–886. [PubMed: 23761323]
18. Demicco EG, Harms PW, Patel RM, et al. Extensive Survey of STAT6 Expression in a Large Series of Mesenchymal Tumors. Am J Clin Pathol. 2015; 143:672–682. [PubMed: 25873501]
19. Doyle LA, Vivero M, Fletcher CD, et al. Nuclear expression of STAT6 distinguishes solitary fibrous tumor from histologic mimics. Mod Pathol. 2014; 27:390–395. [PubMed: 24030747]

20. Hasegawa T, Matsuno Y, Shimoda T, et al. Extrathoracic solitary fibrous tumors: Their histological variability and potentially aggressive behavior. Human Pathology. 1999; 30:1464–1473. [PubMed: 10667425]
21. Gold JS, Antonescu CR, Hajdu C, et al. Clinicopathologic correlates of solitary fibrous tumors. Cancer. 2002; 94:1057–1068. [PubMed: 11920476]
22. Morimitsu Y, Nakajima M, Hisaoka M, et al. Extrapleural solitary fibrous tumor: clinicopathologic study of 17 cases and molecular analysis of the p53 pathway. APMIS. 2000; 108:617–625. [PubMed: 11110050]
23. Brunnemann RB, Ro JY, Ordonez NG, et al. Extrapleural solitary fibrous tumor: a clinicopathologic study of 24 cases. Mod Pathol. 1999; 12:1034–1042. [PubMed: 10574600]
24. Furusato E, Valenzuela IA, Fanburg-Smith JC, et al. Orbital solitary fibrous tumor: encompassing terminology for hemangiopericytoma, giant cell angiofibroma, and fibrous histiocytoma of the orbit: reappraisal of 41 cases. Hum Pathol. 2011; 42:120–128. [PubMed: 21056898]
25. Thompson LD. Sinonasal tract glomangiopericytoma (hemangiopericytoma). Ear Nose Throat J. 2004; 83:807. [PubMed: 15724732]
26. Dandekar M, McHugh JB. Sinonasal glomangiopericytoma: case report with emphasis on the differential diagnosis. Arch Pathol Lab Med. 2010; 134:1444–1449. [PubMed: 20923298]
27. Jo VY, Fletcher CD. Nuclear beta-Catenin Expression is Frequent in Sinonasal Hemangiopericytoma and Its Mimics. Head Neck Pathol. 2016
28. Lewis JT, Oliveira AM, Nascimento AG, et al. Low-grade sinonasal sarcoma with neural and myogenic features: a clinicopathologic analysis of 28 cases. Am J Surg Pathol. 2012; 36:517–525. [PubMed: 22301502]
29. Wang X, Bledsoe KL, Graham RP, et al. Recurrent PAX3-MAML3 fusion in biphenotypic sinonasal sarcoma. Nat Genet. 2014; 46:666–668. [PubMed: 24859338]
30. R Core Team. R: A language and environment for statistical computing. Vienna, Austria: R Foundation for Statistical Computing; 2014.
31. Harrell FE. rms: Regression Modeling Strategies. 2015:4–1. Version R package version 4.
32. Cox DP, Daniels T, Jordan RC. Solitary fibrous tumor of the head and neck. Oral Surg Oral Med Oral Pathol Oral Radiol Endod. 2010; 110:79–84. [PubMed: 20488732]
33. Chan JK. Solitary fibrous tumour--everywhere, and a diagnosis in vogue. Histopathology. 1997; 31:568–576. [PubMed: 9447390]
34. Lau SK, Weiss LM, Chu PG. Myxoid solitary fibrous tumor: a clinicopathologic study of three cases. Virchows Arch. 2009; 454:189–194. [PubMed: 19125290]
35. Cameselle-Teijeiro J, Manuel Lopes J, Villanueva JP, et al. Lipomatous haemangiopericytoma (adipocytic variant of solitary fibrous tumour) of the thyroid. Histopathology. 2003; 43:406–408. [PubMed: 14511266]
36. Tanahashi J, Kashima K, Daa T, et al. Solitary fibrous tumor of the thyroid gland: report of two cases and review of the literature. Pathol Int. 2006; 56:471–477. [PubMed: 16872444]
37. Verdi D, Pennelli G, Pelizzo MR, et al. Solitary fibrous tumor of the thyroid gland: a report of two cases with an analysis of their clinical and pathological features. Endocr Pathol. 2011; 22:165–169. [PubMed: 21818669]
38. Rodriguez I, Ayala E, Caballero C, et al. Solitary fibrous tumor of the thyroid gland: report of seven cases. Am J Surg Pathol. 2001; 25:1424–1428. [PubMed: 11684960]
39. McDaniel AS, Palanisamy N, Smith SC, et al. A Subset of Solitary Fibrous Tumors Express Nuclear PAX8 and PAX2: a Potential Diagnostic Pitfall. Histol Histopathol.
40. Nonaka D, Tang Y, Chiriboga L, et al. Diagnostic utility of thyroid transcription factors Pax8 and TTF-2 (FoxE1) in thyroid epithelial neoplasms. Mod Pathol. 2008; 21:192–200. [PubMed: 18084247]
41. Pang KP, Chee LW, Busmanis I. Amyloidoma of the nose in a pediatric patient: a case report. American journal of otolaryngology. 2001; 22:138–141. [PubMed: 11283830]
42. Enzinger FM, Smith BH. Hemangiopericytoma: An analysis of 106 cases. Human Pathology. 1976; 7:61–82. [PubMed: 1244311]

43. McMaster MJ, Soule EH, Ivins JC. Hemangiopericytoma: A clinicopathologic study and long-term followup of 60 patients. Cancer. 1975; 36:2232–2244. [PubMed: 1203874]
44. Middleton LP, Duray PH, Merino MJ. The histological spectrum of hemangiopericytoma: application of immunohistochemical analysis including proliferative markers to facilitate diagnosis and predict prognosis. Hum Pathol. 1998; 29:636–640. [PubMed: 9635686]
45. Vallat-Decouvelaere AV, Dry SM, Fletcher CD. Atypical and malignant solitary fibrous tumors in extrathoracic locations: evidence of their comparability to intra-thoracic tumors. Am J Surg Pathol. 1998; 22:1501–1511. [PubMed: 9850176]
46. Demicco EG, Park MS, Araujo DM, et al. Solitary fibrous tumor: a clinicopathological study of 110 cases and proposed risk assessment model. Mod Pathol. 2012; 25:1298–1306. [PubMed: 22575866]
47. Smith SC, Patel RM, Lucas DR, et al. Sinonasal lobular capillary hemangioma: a clinicopathologic study of 34 cases characterizing potential for local recurrence. Head Neck Pathol. 2013; 7:129–134. [PubMed: 23184353]
48. Bowe SN, Wakely PE Jr, Ozer E. Head and neck solitary fibrous tumors: diagnostic and therapeutic challenges. Laryngoscope. 2012; 122:1748–1755. [PubMed: 22549404]
49. Ganly I, Patel SG, Stambuk HE, et al. Solitary fibrous tumors of the head and neck: a clinicopathologic and radiologic review. Archives of otolaryngology--head & neck surgery. 2006; 132:517–525. [PubMed: 16702568]
50. Kunzel J, Hainz M, Ziebart T, et al. Head and neck solitary fibrous tumors: a rare and challenging entity. Eur Arch Otorhinolaryngol. 2015
51. Kao YC, Lin PC, Yen SL, et al. Clinicopathological and genetic heterogeneity of the head and neck solitary fibrous tumours: a comparative histological, immunohistochemical and molecular study of 36 cases. Histopathology. 2016; 68:492–501. [PubMed: 26154686]
52. Yang XJ, Zheng JW, Ye WM, et al. Malignant solitary fibrous tumors of the head and neck: a clinicopathological study of nine consecutive patients. Oral Oncol. 2009; 45:678–682. [PubMed: 19147392]

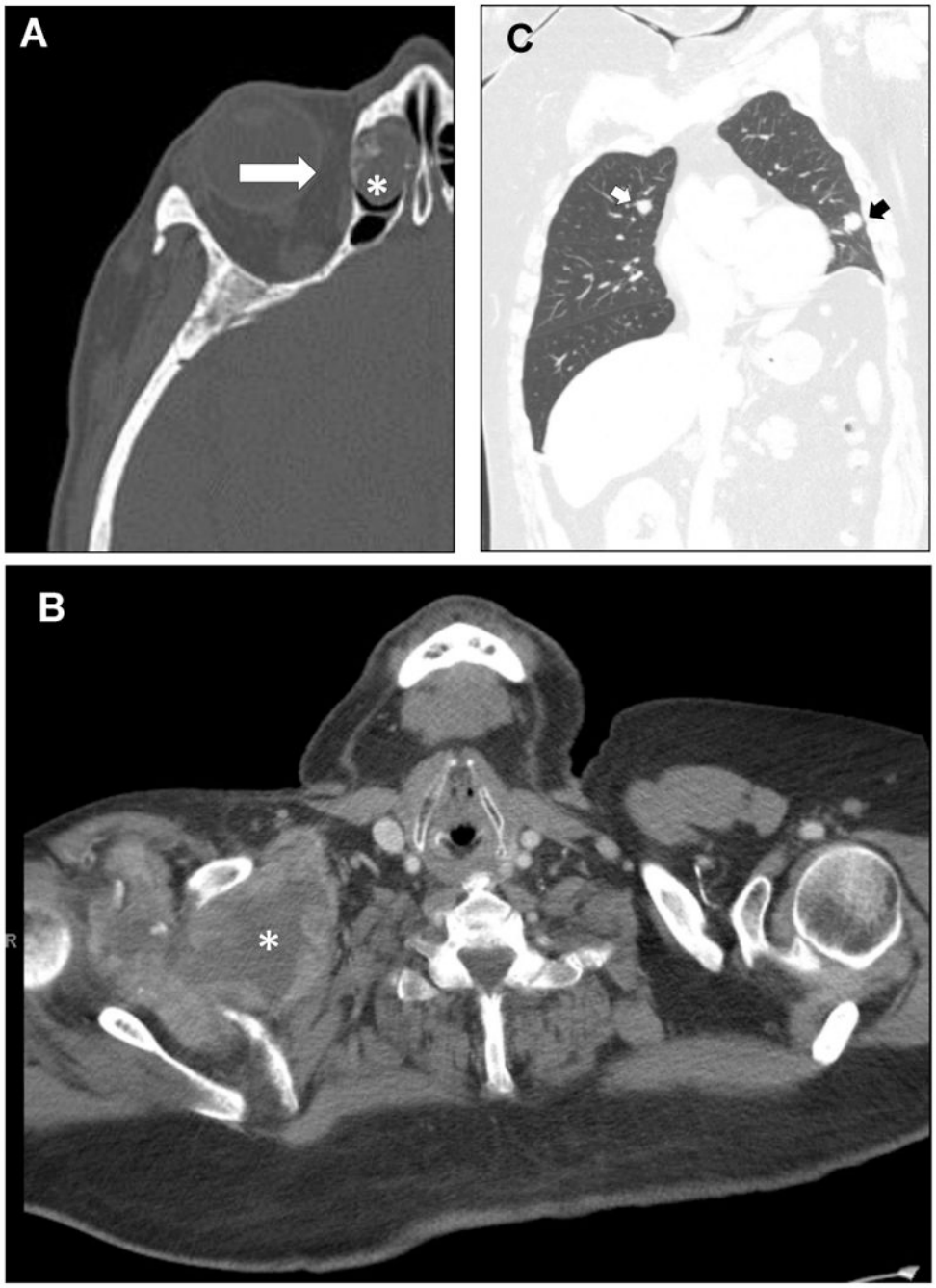

Figure 1.

Imaging findings for head and neck SFTs. A. The sinonasal tract was the most prevalent site of involvement, this CT scan showing a tumor based in the nasal cavity invading the ethmoidal cells (lesion, *) with erosion into the orbit (arrow). B. A single SFT with sarcomatous dedifferentiation arose in the base of the neck (*) and extending caudad through the level of the thyroid cartilage. C. Pulmonary metastases (arrows) were observed.

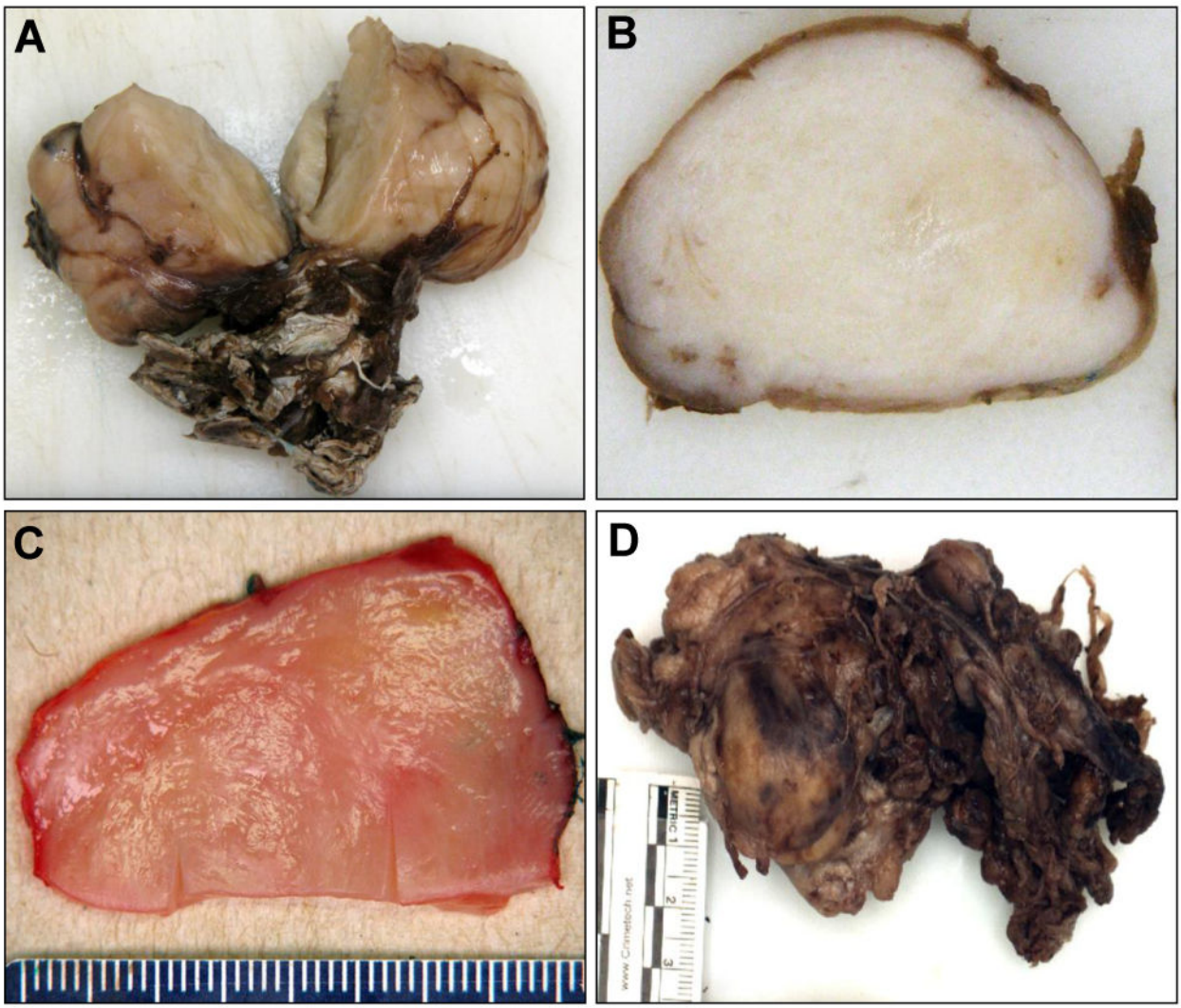

Figure 2.

Gross findings for head and neck SFTs. A. A classic SFT, arising in a pediatric patient, demonstrated a typical indurated, fibrous, well-circumscribed but unencapsulated appearance, with attached soft tissue. B. Another classic SFT, which showed a whorled pattern microscopically, was grossly reminiscent of a leiomyoma. C. A cellular SFT with myxoid and lipomatous differentiation showed a soft, pink, “fish flesh” appearance. D. The single dedifferentiated SFT, in contrast, showed an irregular, multinodular appearance, infiltrating the attached skeletal muscle.

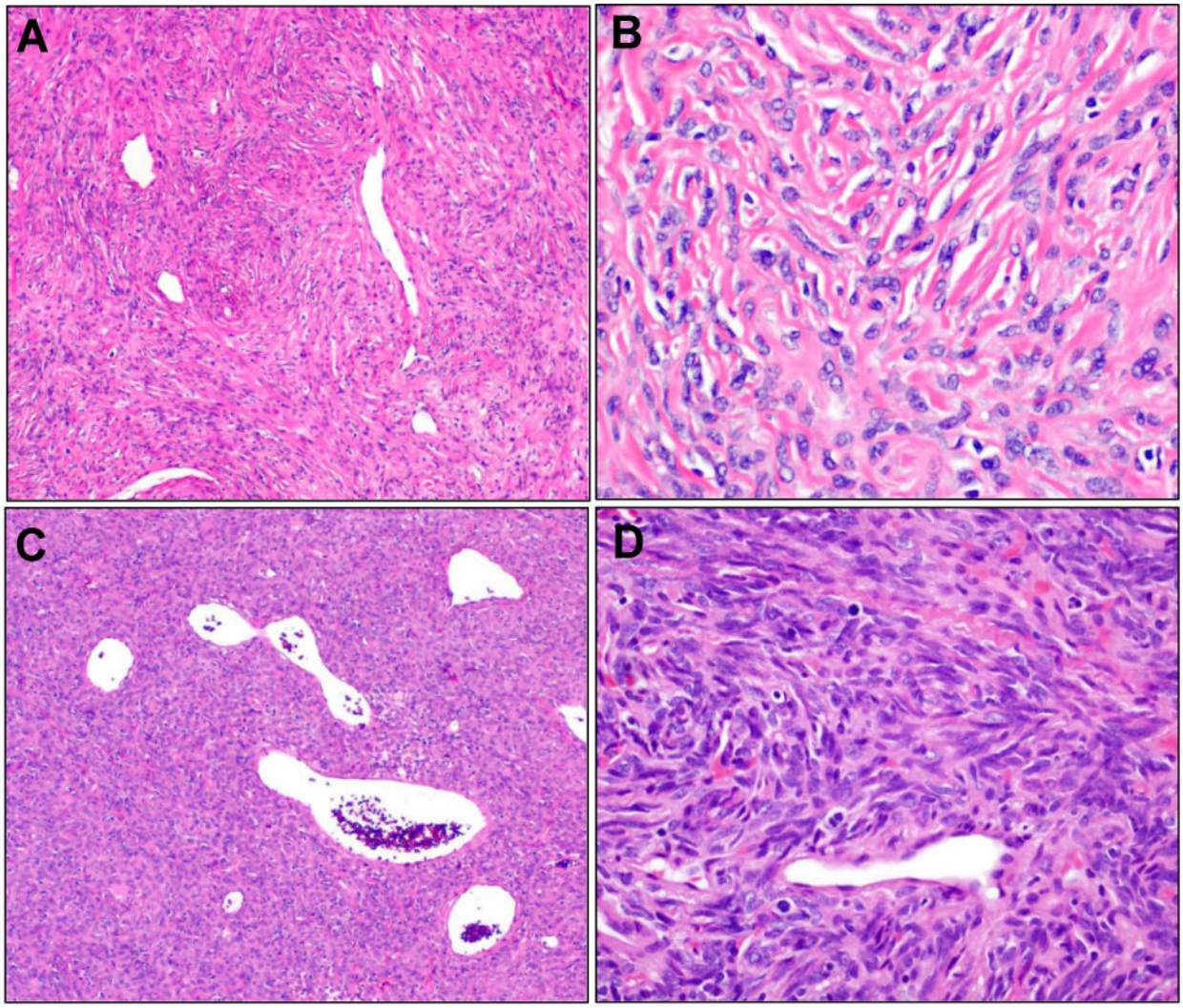

Figure 3.

Microscopic findings for classic and cellular SFTs. A. A case previously designated OFH showed a classic SFT pattern with low to intermediate cellularity, densely collagenized, with “staghorn” vasculature. B. At higher power, the tumor from A showed bland ovoid to fusiform cells are apparent, intimately admixed with the collagenized stroma, with indistinct borders, ovoid to angulated nuclei, and evenly distributed chromatin. C. A case previously designated HPC shows the cellular SFT pattern, a cellular, darker lesion, with the characteristic vessels. D. At higher power, the tumor from C shows dense, patternless arrays of cells, cytologically indistinguishable from those of a classic SFT.

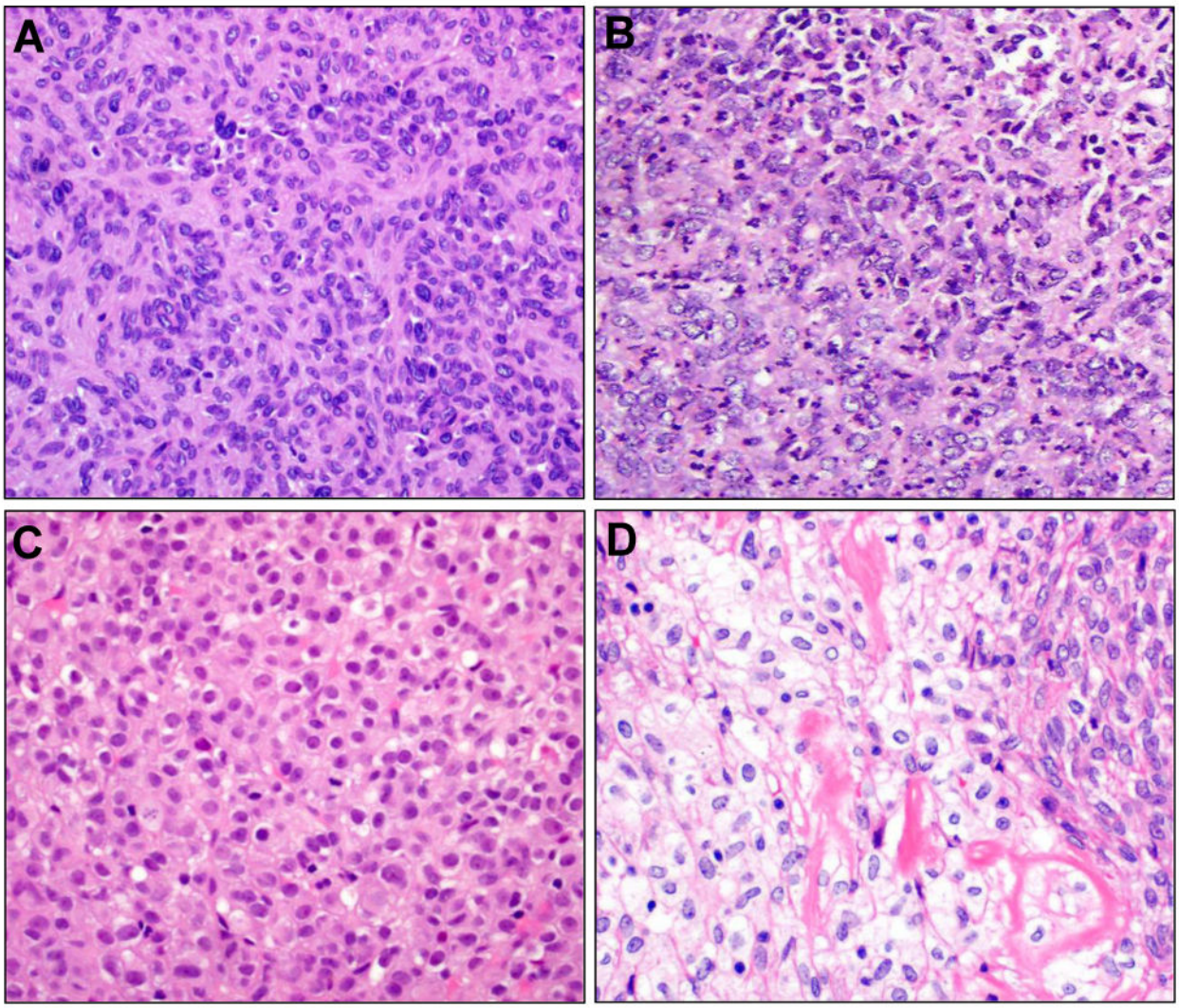

Figure 4.

Cellular atypia was defined as nuclear pleomorphism, often overlapping (A) or if markedly irregular/vesicular chromatin were present (B, lower left). In this case, coagulative tumor cell necrosis (upper right corner) was present. Epithelioid cytomorphology (C) was defined by a pervasive morphology of remarkably plump, round cells with pale to eosinophilic cytoplasm and central nuclei with readily identified nucleoli. Only one case demonstrated widely scattered foci of explicit clear cell change imparting a focal impression of epithelioid features (D), distinct from the otherwise conventional morphology (upper right). Such focal changes were not considered epithelioid.

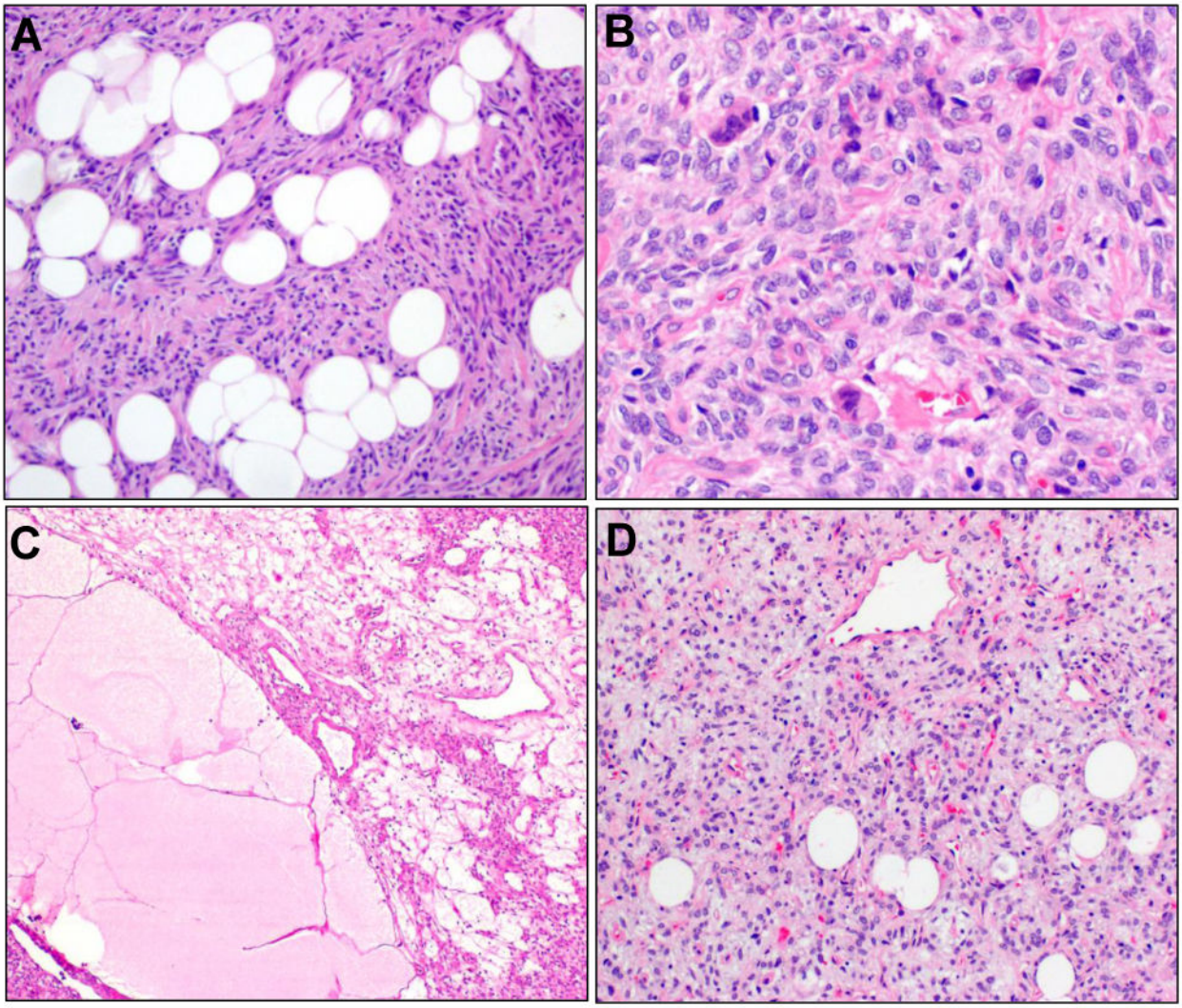

Figure 5.

A. Lipomatous differentiation was present in both classic SFTs (seen here) and cellular SFTs. B. SFTs with stromal giant cells (arrows), as previously designated as GCA were infrequent. C. Myxoid change was seen in a subset, associated with microcystic change, and myxoid pools with pulmonary edema-like appearance (lower left). D. Stromal myxoid change, with concomitant lipomatous differentiation, had raised consideration of myxoid liposarcoma in a biopsy sample.

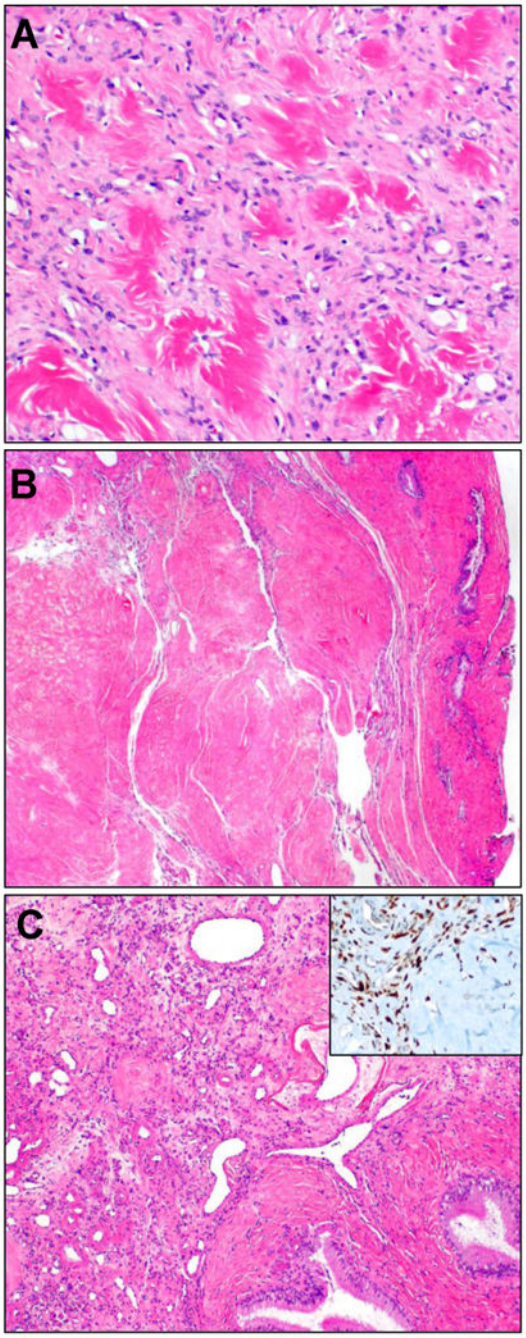

Figure 6.

Prominent stromal hyalinization, in association with vessels and in the stroma, imparted the appearance of collagen rosettes (A) with the appearance of amianthoid fibers or keloidal collagen. In one case, this feature predominated (B), such that a nodular amyloidoma had entered the differential. Upon close inspection, distinctive SFT vasculature was apparent (C), and STAT6 was positive (inset).

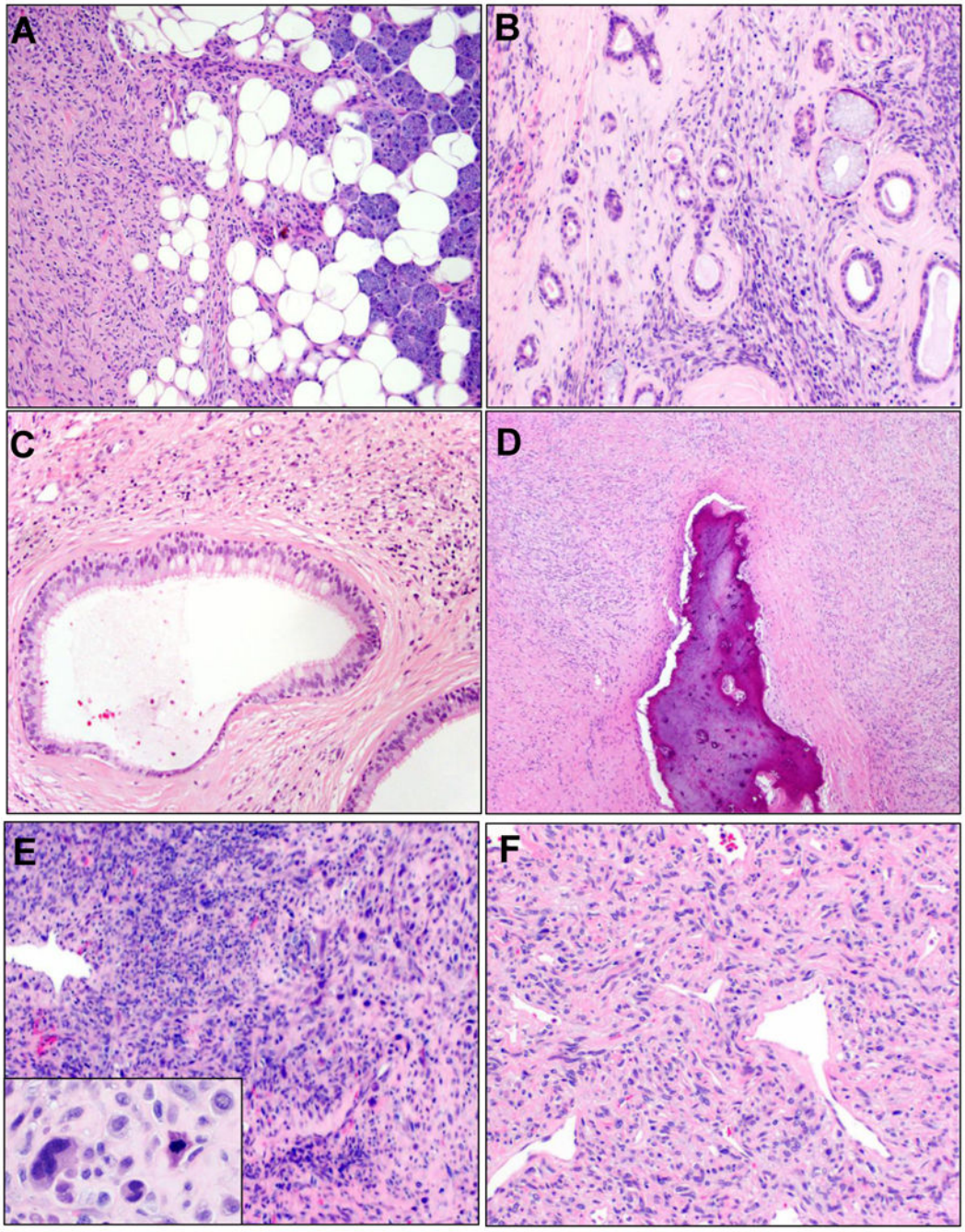

Figure 7.

Invasion and dedifferentiation. Invasion of adjacent organs (A, parotid gland) and entrapment of epithelial ductal elements (B) were deemed to represent infiltrative growth. In some sinonasal SFTs, cystic dilatation of entrapped glands and ducts imparted an almost biphasic appearance (C). Osseous invasion was noted in many SFTs where bone was resected (D). Dedifferentiation was present in one SFT as overtly sarcomatous overgrowth with frank cytologic pleomorphism (E) and necrosis (other fields); other areas of the tumor showed classic SFT morphology with obvious nuclear atypia (F).

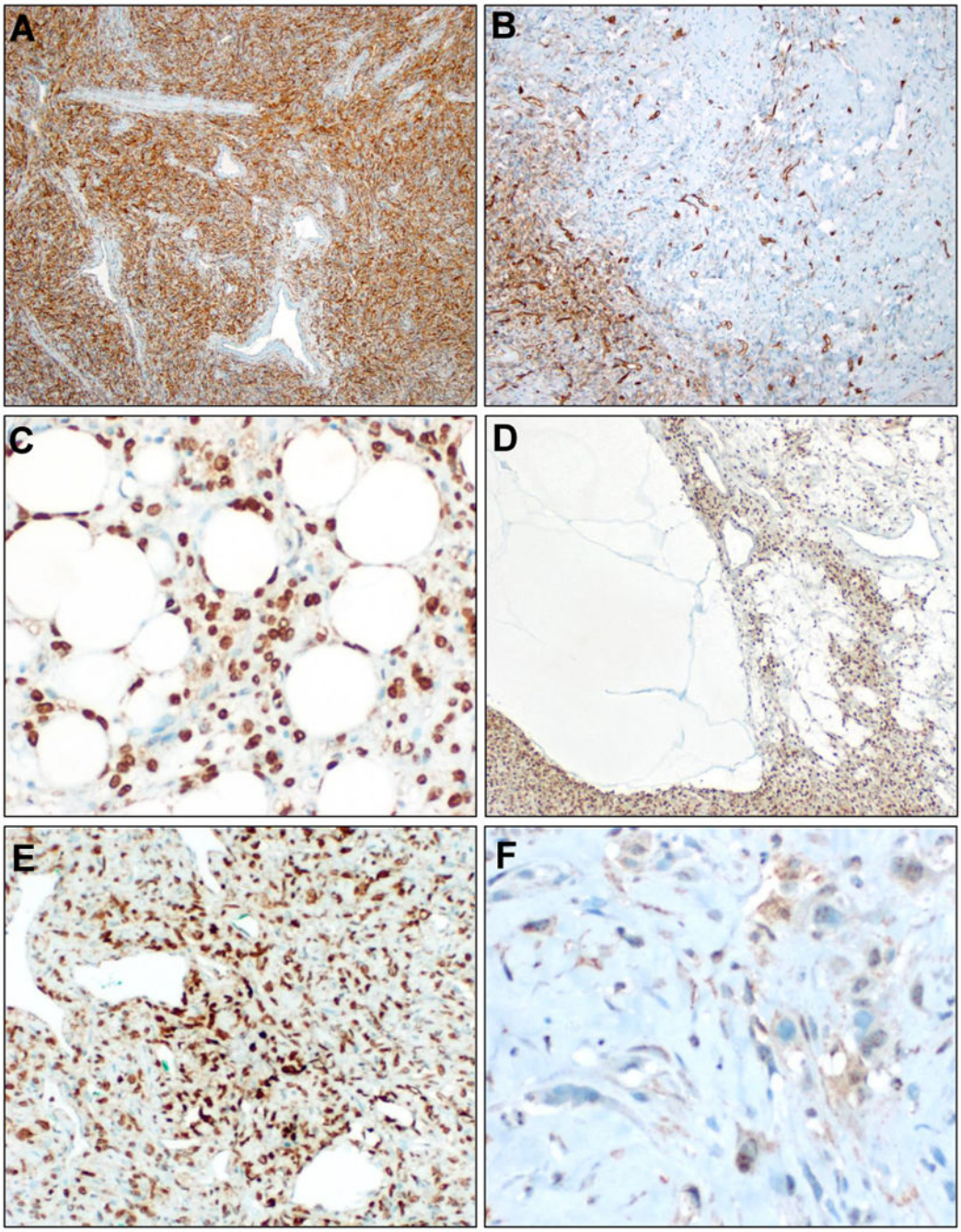

Figure 8.

Immunophenotype. CD34 immunostain was positive in >90% of SFTs, approximately half diffusely (A), half multifocally. (B). STAT6 was diffuse nuclear positive in all cases studied, including SFTs with lipomatous differentiation (C) or myxoid change (D). In the dedifferentiated SFT, STAT6 positivity was diffuse in the conventional SFT component (E) but markedly decreased in the sarcomatous component (F).

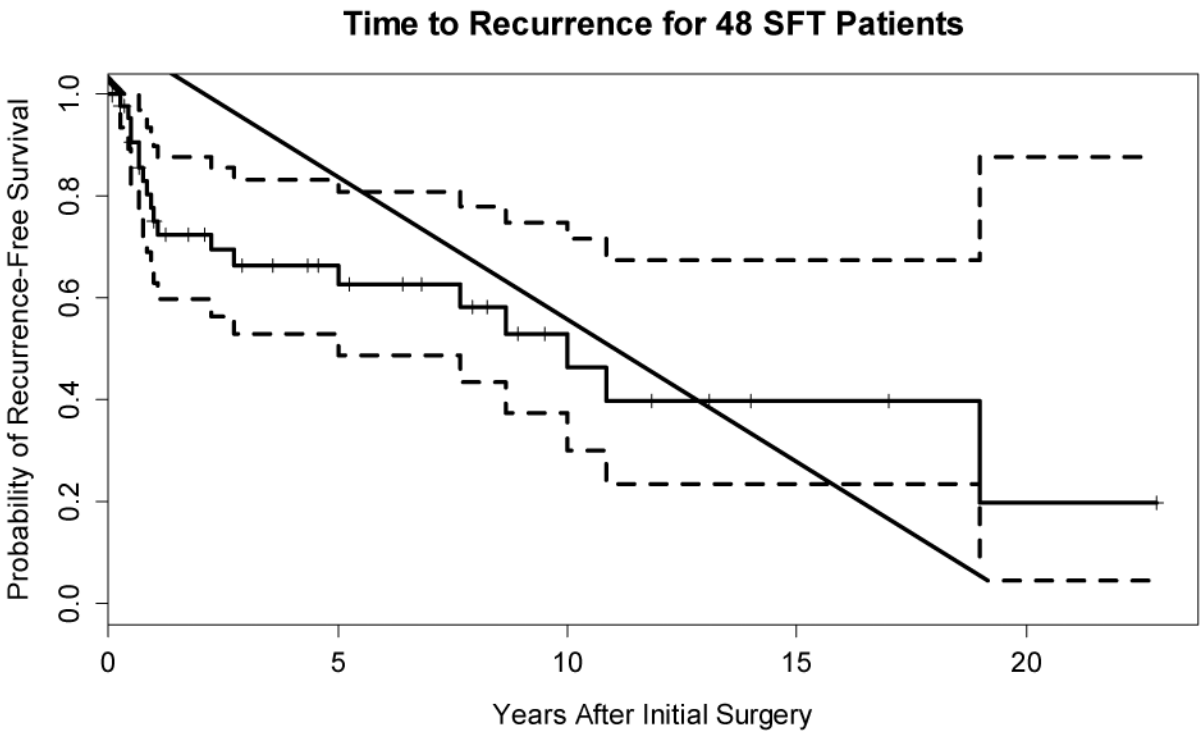

Figure 9.

Kapan – Meier plot of the probability of being free of recurrence. The dashed lines are 95% confidence bands; the vertical tick marks denote time of censoring.

Table 1

Clinicopathologic Features of Solitary Fibrous Tumors of the Head and Neck, including Recurrence Status

Case	Sex	Age [y]	Site	Original Dx	Size [cm]	Rec. Size [cm]	Morphology	Atypia	Epithelioid	Mits/10HPF	Necrosis	Rec. Status	Time to Rec. [mo]
SFT1	F	30	sinonasal	SFT	0.9	NA	classic	N	N	0	N	NED	94.7
SFT2	F	54	sinonasal	SFT	8	9	classic	N	N	4	N	REC	60.0
SFT3	F	49	salivary gland	SFT	4	LTF	classic	N	N	1	N	LTF	LTF
SFT4	F	59	sinonasal	SFT	2.5	0.4	classic	N	N	1	N	REC	6.4
SFT5	F	70	sinonasal	SFT	3	NA	classic	N	N	2	N	NED	2.9
SFT6	M	16	orbital	SFT	2.9	NA	classic	N	N	0	N	NED	25.3
SFT7	F	50	orbital	SFT	3	LTF	cellular	N	N	6	N	LTF	LTF
SFT8	M	46	orbital	SFT	3.4	NA	classic	N	N	3	N	NED	51.8
SFT9	F	>89	orbital	SFT	~	LTF	classic	N	N	2	N	LTF	LTF
SFT10	M	34	orbital	SFT	~	LTF	classic	N	N	0	N	LTF	LTF
SFT11	F	56	sinonasal	SFT	2.7	5.5	cellular	N	N	8	N	REC	32.9
SFT12	M	42	salivary gland	SFT	6.5	LTF	cellular	N	N	0	N	LTF	LTF
SFT13	F	48	neck soft tissue	SFT	8	LTF	classic	N	N	0	N	NED	20.5
SFT14	M	48	orbital	SFT	~	LTF	cellular	Y	N	6	N	LTF	LTF
SFT15	M	28	orbital	HPC	1.2	LTF	cellular	N	N	1	N	LTF	LTF
SFT16	F	88	neck soft tissue	HPC	5.3	NA	cellular	N	N	0	N	NED	34.6
SFT17	F	34	sinonasal	HPC	2.2	4.5	cellular	N	Y	6	N	REC	103.5
SFT18	F	17	subcutaneous	HPC	3	NA	cellular	Y	N	7	Y	NED	3.5
SFT19	M	63	sinonasal	HPC	4	4	cellular	N	N	5	N	REC	228.0
SFT20	M	30	orbital	HPC	0.7	NA	cellular	N	Y	7	N	NED	142.3
SFT21	F	41	sinonasal	HPC	9.7	10	cellular	Y	N	4	N	REC	92.0
SFT22	M	36	sinonasal	HPC	4	NA	cellular	N	N	0	N	NED	1.2
SFT23	F	41	orbital	HPC	4.5	5	classic	N	N	1	N	REC	12.0
SFT24	F	60	orbital	OFH	0.4	NA	cellular	N	N	1	N	NED	106.8
SFT25	M	45	orbital	OFH	1.7	NA	classic	N	N	1	N	NED	157.3
SFT26	F	31	subcutaneous	OFH	0.6	NA	cellular	N	N	2	N	NED	43.2

Case	Sex	Age [y]	Site	Original Dx	Size [cm]	Rec. Size [cm]	Morphology	Atypia	Epithelioid	Mits/10HPF	Necrosis	Rec. Status	Time to Rec. [mo]
SFT27	M	26	subcutaneous	OFH	0.7	NA	classic	N	N	1	N	NED	6.3
SFT28	F	63	sinonasal	SFT	2.8	NA	classic	N	N	0	N	NED	1.0
SFT29	F	16	oral cavity	SFT	5.1	NA	classic	N	N	0	N	NED	0.3
SFT30	M	58	orbital	SFT	4.3	NA	classic	N	N	1	N	REC	9.0
SFT31	M	22	orbital	HPC	1.6	LTF	cellular	N	N	0	N	LTF	LTF
SFT32	M	55	salivary gland	HPC	1.5	NA	classic	N	N	0	N	NED	274.0
SFT33	M	58	orbital	HPC	~	5.5	cellular	N	N	0	N	REC	120.0
SFT34	F	52	oral cavity	HPC	1.7	NA	cellular	N	N	0	N	NED	204.0
SFT35	F	49	subcutaneous	HPC	6	LTF	cellular	Y	N	1	N	LTF	LTF
SFT36	M	59	ear	SFT	~	LTF	classic	N	N	0	N	LTF	LTF
SFT37	F	52	salivary gland	SFT	2	LTF	classic	N	N	0	N	LTF	LTF
SFT38	F	74	sinonasal	SFT	4	NA	classic	N	N	0	N	NED	114.0
SFT39	F	70	salivary gland	SFT	2.5	LTF	cellular	Y	N	4	N	LTF	LTF
SFT40	F	27	oral cavity	SFT	~	LTF	cellular	Y	N	7	N	LTF	LTF
SFT41	M	55	orbital	SFT	~	LTF	cellular	N	Y	1	N	LTF	LTF
SFT42	M	49	oral cavity	SFT	~	LTF	classic	N	N	1	N	LTF	LTF
SFT43	M	39	orbital	SFT	~	~	cellular	Y	Y	0	N	REC	27.0
SFT44	F	38	orbital	SFT	2.8	LTF	cellular	N	Y	2	N	LTF	LTF
SFT45	F	50	sinonasal	SFT	~	2.7	classic	N	N	0	N	REC	8.0
SFT46	M	66	oral cavity	SFT	~	LTF	classic	N	N	0	N	LTF	LTF
SFT47	M	66	oral cavity	SFT	2	LTF	cellular	Y	N	1	N	LTF	LTF
SFT48	M	67	oral cavity	SFT	2.8	LTF	classic	N	Y	3	N	LTF	LTF
SFT49	F	60	oral cavity	SFT	1.5	NA	classic	N	N	0	N	NED	77.0
SFT50	F	41	sinonasal	SFT	~	LTF	cellular	N	N	1	N	LTF	LTF
SFT51	F	52	sinonasal	SFT	~	LTF	classic	N	N	0	N	LTF	LTF
SFT52	M	42	oral cavity	SFT	~	LTF	classic	N	N	0	N	LTF	LTF
SFT53	M	47	sinonasal	HPC	~	5.5	cellular	Y	Y	10	N	REC	130.0
SFT54	F	47	salivary gland	SFT	1	NA	classic	N	N	0	N	NED	62.5
SFT55	F	44	salivary gland	SFT	2.2	LTF	cellular	N	N	0	N	LTF	LTF

Case	Sex	Age [y]	Site	Original Dx	Size [cm]	Rec. Size [cm]	Morphology	Atypia	Epithelioid	Mits/10HPF	Necrosis	Rec. Status	Time to Rec. [mo]
SFT56	F	84	neck soft tissue	SFT	9	NA	cellular	Y	~	~	Y	NED	12.0
SFT57	F	85	oral cavity	SFT	2.3	~	cellular	Y	Y	5	N	REC	8.0
SFT58	F	54	sinonasal	SFT	~	NA	classic	N	N	0	N	LTF	LTF
SFT59	M	77	salivary gland	SFT	3.3	NA	cellular	N	N	4	Y	LTF	LTF
SFT60	M	64	subcutaneous	SFT	3.2	5	cellular	N	N	2	N	REC	11.0
SFT61	F	64	sinonasal	SFT	2.6	~	classic	N	N	0	N	LTF	LTF
SFT62	F	52	neck soft tissue	SFT	5	~	cellular	Y	Y	18	Y	REC	12.7
SFT63	M	31	orbital	SFT	~	~	classic	N	N	0	N	LTF	LTF
SFT64	M	82	sinonasal	SFT/GCA	~	~	classic	N	N	0	N	LTF	LTF
SFT65	F	65	sinonasal	SFT	~	~	classic	N	N	0	N	LTF	LTF
SFT66	M	78	sinonasal	SFT	~	~	cellular	Y	~	~	~	LTF	LTF
SFT67	F	85	neck soft tissue	SFT	1.5	NA	cellular	N	~	~	~	LTF	LTF
SFT68	F	72	neck soft tissue	HPC	~	4.5	cellular	Y	Y	0	N	REC	4.9
SFT69	M	64	subcutaneous	SFT	3.2	LTF	classic	Y	N	6	N	LTF	LTF
SFT70	M	62	neck soft tissue	SFT	8	~	cellular	Y	Y	18	Y	REC	2.6
SFT71	F	38	oral cavity	SFT	2.8	NA	classic	N	N	6	N	NED	7.8
SFT72	M	28	orbital	OFH/GCA	3	LTF	classic	N	N	0	N	LTF	LTF
SFT73	M	50	sinonasal	SFT	4	LTF	classic	N	N	0	N	LTF	LTF
SFT74	M	37	orbital	OFH	3	LTF	classic	N	N	0	N	LTF	LTF
SFT75	M	39	sinonasal	SFT	2	LTF	classic	N	N	0	N	LTF	LTF
SFT76	F	69	sinonasal	SFT	2.7	NA	classic	N	N	1	N	NED	82.0
SFT77	M	56	neck soft tissue	SFT	6	NA	classic	N	N	0	N	NED	54.6
SFT78	M	44	sinonasal	SFT	7.5	LTF	classic	N	N	0	N	LTF	LTF
SFT79	F	39	salivary gland	SFT	3.5	LTF	classic	N	N	0	N	LTF	LTF
SFT80	M	51	sinonasal	HPC	2	NA	cellular	N	N	1	N	NED	4.0
SFT81	F	66	orbital	HPC	2.7	NA	classic	Y	N	2	N	NED	15.0
SFT82	M	52	salivary gland	HPC	5.5	NA	cellular	Y	Y	4	N	NED	168.0
SFT83	M	52	salivary gland	HPC	3.5	NA	cellular	N	N	0	N	NED	99.0
SFT84	F	42	salivary gland	HPC	~	3.1	cellular	Y	Y	6	N	REC	10.0

Case	Sex	Age [y]	Site	Original Dx	Size [cm]	Rec. Size [cm]	Morphology	Atypia	Epithelioid	Mits/10HPF	Necrosis	Rec. Status	Time to Rec. [mo]
SFT85	F	15	orbital	HPC	~	1.7	cellular	Y	N	8	N	REC	6.0
SFT86	F	68	sinonasal	SFT	2.8	2.8	classic	N	N	0	N	NED	6.0
SFT87	F	59	oral cavity	SFT	1.1	LTF	classic	N	N	0	N	LTF	LTF
SFT88	F	78	oral cavity	SFT	0.9	LTF	classic	N	N	0	N	LTF	LTF

Abbreviations: ~, no data; M, male; F, female; SFT, solitary fibrous tumor; HPC, hemangiopericytoma; OFH, orbital fibrous histiocytoma; GCA, giant cell angiofibroma; NA, not applicable; Rec., recurrence; LTF, lost to follow-up; NED, no evidence of disease; REC, recurrence noted in follow-up; Mits./10HPF, mitoses per 10 high power fields.

Table 2

Immunohistochemical Findings*

Marker	Negative N(%)	Focal/Multifocal N(%)	Diffuse N(%)	Total
CD34	7 (9)	32 (40)	41 (51)	80
S100	58 (95)	3 (5)	~	61
SMA	42 (84)	8 (16)	~	50
Pan-Cytokeratins	48 (96)	2 (4)	~	50
BCL2	3 (8)	36 (90)	1 (3)	40
CD99	2 (6)	29 (94)	~	31
EMA	22 (92)	2 (8)	~	24
	Negative N (%)		Positive N (%)	
STAT6	0		45 (100%)	

*Archival immunostains were reviewed tabulated if interpretable for the markers listed, excepting UMHS cases where CD34 was performed on all cases with evaluable material (see Methods). STAT6 immunostains were performed at UMHS on all CSMC and VCUHS cases as well as a subset of UMHS cases for this study. UPMC cases with available material were stained for STAT6 as described. Additional IHC findings per evaluation of original archived immunostains. ~, none observed.

Table 3

Analysis of Potential Risk Factors for Recurrence of SFT

Covariate	N	Reference	Hazard Ratio	95% Confidence Interval	P
Gender: Male	48	Female	0.5	.018 – 1.43	0.20
Age [y]	48	40 – 62	1.05	.52 – 2.13	0.88
Original diagnosis	48	SFT			0.46
HPC			.52	.18 – 1.5	
OFH			0		
Institution	48	UMHS			0.84
CSMC			1.03	.22 – 4.89	
UPMC			1.11	.40 – 3.08	
VCUHS			2.09	.43 – 10.12	
Size	41	2 – 4.5	1.68	1.01 – 2.78	**0.04**
Site	48	Sinonasal			0.68
Neck Soft Tissue			1.44	.35 – 5.90	
Oral Cavity			.48	.06 – 3.93	
Orbital			.79	.25 – 2.48	
Salivary Gland			.22	.03 – 1.75	
Subcutaneous			1.12	.13 – 9.44	
Morphology: Cellular	48	Classic SFT	2.10	.75 – 5.89	0.16
Atypia	48	No Atypia	3.44	1.36 – 8.73	**0.01**
Epithelioid	48	No Epithelioid	2.56	.99 – 6.56	**0.05**
Mitotic Index	48	0 – 4.25	1.67	1.16 – 2.41	**0.01**
Necrosis	48	No necrosis	4.98	1.31 – 18.95	**0.02**
Infiltrative	41	Not Infiltrative	2.21	.77 – 6.36	0.14

Covariate	N	Reference	Hazard Ratio	95% Confidence Interval	P
Positive Margin	35	Negative Margin	2.65	.58 – 12.11	0.21

Abbreviations: SFT, solitary fibrous tumor; HPC, hemangiopericytoma; OFH, orbital fibrous histiocytoma; N, number with available data for analysis; P, P-values for association with time to recurrence by Cox proportional hazards regression analysis.